

Structural assignments of NMR chemical shifts in $\text{Ge}_x\text{Se}_{1-x}$ glasses via first-principles calculations for GeSe_2 , Ge_4Se_9 , and GeSe crystals

Mikhail Kibalchenko,¹ Jonathan R. Yates,² Carlo Massobrio,³ and Alfredo Pasquarello^{4,5}

¹*TCM Group, Cavendish Laboratory, University of Cambridge, Cambridge CB3 0HE, United Kingdom*

²*Department of Materials, University of Oxford, Oxford OX1 3PH, United Kingdom*

³*Institut de Physique et de Chimie des Matériaux de Strasbourg, 23 rue du Loess, BP 43, F-67034 Strasbourg Cedex 2, France*

⁴*Institute of Theoretical Physics, Ecole Polytechnique Fédérale de Lausanne (EPFL), CH-1015 Lausanne, Switzerland*

⁵*Institut Romand de Recherche Numérique en Physique des Matériaux (IRRMA), CH-1015 Lausanne, Switzerland*

(Received 3 June 2010; published 30 July 2010)

Structural assignments are determined for ^{77}Se and ^{73}Ge chemical shifts through density-functional NMR calculations for GeSe_2 , Ge_4Se_9 , and GeSe crystals. In particular, a very good agreement between calculated and measured ^{77}Se isotropic chemical shifts and anisotropies is found for the GeSe_2 crystal, for which experimental data are available. These assignments provide a consistent interpretation of experimental ^{77}Se spectra of $\text{Ge}_x\text{Se}_{1-x}$ glasses, indicating that the contribution from Ge-Se-Se linkages overlaps with that from Ge-Se-Ge linkages in corner-sharing tetrahedral arrangements, thereby dismissing the occurrence of a bimodal phase.

DOI: 10.1103/PhysRevB.82.020202

PACS number(s): 61.43.Fs, 76.60.-k, 71.15.Mb

Chalcogenide glasses are sensitive to the absorption of electromagnetic radiation and show a variety of photoinduced effects.¹ These properties show potential for numerous applications in active and passive optics.² Thus, chalcogenide $\text{Ge}_x\text{Se}_{1-x}$ glasses are currently under intense experimental and theoretical investigations to elucidate their structural arrangement. For $\text{Ge}_x\text{Se}_{1-x}$ glasses, conventional diffraction probes are not sufficient for providing a complete determination of the short-range order,³ which include corner-sharing (CS) and edge-sharing (ES) tetrahedral arrangements,⁴ undercoordinated and overcoordinated atoms,⁵⁻⁷ and homopolar bonds.⁴ Raman spectroscopy can also act as a structural probe providing for instance indications about the relative populations of corner-sharing and edge-sharing tetrahedra but relies on theoretical estimates of coupling factors.³

Recently, the short-range structure in $\text{Ge}_x\text{Se}_{1-x}$ glasses has been studied by solid state nuclear magnetic resonance (NMR).⁸⁻¹⁰ The measured ^{77}Se NMR spectra mainly consist of two different peaks but conflicting conclusions have been reached about their interpretation. One of the invoked models is based on the occurrence of a bimodal phase in which the two phases only bond weakly and are characterized by Se-Se-Se and Ge-Se-Ge sites, respectively.^{8,9} The other interpretation scheme relies on NMR measurements for crystalline GeSe_2 and assumes that the structure is fully bonded with intermediate configurations giving rise to overlapping contributions.¹⁰ The latter scheme is also supported by *ab initio* molecular-dynamics simulations on Ge-Se (Refs. 6 and 7) and Ge-Te (Ref. 11) systems. This situation highlights the need for a reliable assignment scheme to relate ^{77}Se chemical shifts to bonding configurations.

In this work, we provide structural assignments for ^{77}Se NMR chemical shifts based on density-functional calculations of NMR parameters of GeSe_2 , Ge_4Se_9 , and GeSe crystals. The reliability of our calculated results is demonstrated for the GeSe_2 crystal, for which experimental data are available.¹⁰ The proposed assignments support an interpretation of experimental ^{77}Se spectra of $\text{Ge}_x\text{Se}_{1-x}$ glasses⁸⁻¹⁰

based on overlapping contributions from various bonding configurations and do not support the occurrence of a bimodal phase.

Magnetic shielding and electric field gradient (EFG) tensors were calculated for crystal GeSe_2 ,¹² Ge_4Se_9 ,¹³ and GeSe (Ref. 14) structures using the gauge including projector augmented wave¹⁵ approach implemented in the CASTEP code.^{16,17} This approach uses periodic boundary conditions, which makes it applicable to crystalline systems. The CASTEP code uses a plane-wave-basis implementation of the density-functional theory. All calculations were carried out using ultrasoft pseudopotentials¹⁸ with the Perdew-Burke-Ernzerhof¹⁹ exchange-correlation functional and a maximum plane-wave energy of 500 eV. The Brillouin zone was sampled using a Monkhorst-Pack²⁰ grid with a maximum density of up to $14 \times 18 \times 18$ k points. These parameters were chosen to converge the results to within 1 ppm for ^{77}Se and ^{73}Ge shieldings and within 0.1 MHz for ^{73}Ge quadrupole coupling constants. Isotropic shieldings σ_{iso} , were calculated for each atom in the considered models. Experiment provides the isotropic chemical shift δ_{iso} which is defined relative to a reference shielding σ_{ref} such that $\delta_{\text{iso}} = -(\sigma_{\text{iso}} - \sigma_{\text{ref}})$. We used $\sigma_{\text{ref}} = 1494$ ppm for ^{77}Se and $\sigma_{\text{ref}} = 1215$ ppm for ^{73}Ge . The reference value for ^{77}Se ensures that the average calculated shieldings for the GeSe_2 crystal coincide with that of the measured ones.¹⁰ The validity of this reference value was independently confirmed for the Se crystal (Ref. 21), for which we calculated a ^{77}Se chemical shift of 824 ppm with the same reference, in excellent agreement with the experimental value of 809 ppm (Ref. 22). For ^{73}Ge , the reference value was chosen to reproduce the experimental value of the shielding in α quartz GeO_2 , $\delta_{\text{iso}} = -110$ ppm (Ref. 23), in accord with a previous NMR study on GeO_2 .²⁴ The chemical shift anisotropy Δ_{cs} was obtained from the calculated chemical shielding tensor using $\Delta_{\text{cs}} = -(\sigma_{33} - \sigma_{\text{iso}})$, where the principal components of the chemical shielding tensor σ_{11} , σ_{22} , and σ_{33} were ordered such that

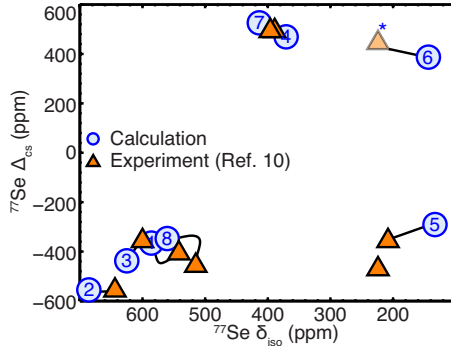


FIG. 1. (Color online) ^{77}Se chemical shift anisotropy (Δ_{cs}) vs isotropic chemical shift (δ_{iso}) for ^{77}Se atoms of the GeSe_2 crystal: present theory (circles) and experiment of Ref. 10 (triangles). Connections between the calculated and measured results indicate our suggested assignments. The asterisk indicates one data point obtained through sign inversion of the measured anisotropy. The labeling is taken from Ref. 12.

$$|\sigma_{33} - \sigma_{\text{iso}}| \geq |\sigma_{11} - \sigma_{\text{iso}}| \geq |\sigma_{22} - \sigma_{\text{iso}}|. \quad (1)$$

We note that Δ_{cs} does not depend on the choice of σ_{ref} . We obtained the quadrupole coupling constant C_Q for ^{73}Ge from the EFG tensor,²⁵ by taking the value of $19.60 \times 10^{-30} \text{ m}^2$ (Ref. 26) for the quadrupole moment.

We first addressed isotropic chemical shifts for each Se site in the GeSe_2 crystal,¹² for which experimental NMR spectra were recently obtained.¹⁰ The horizontal axis in Fig. 1 allows one to compare calculated isotropic chemical shift δ_{iso} with the experimental data of Ref. 10. The calculated and measured shifts agree within the experimental accuracy, leading to a straightforward assignment (Fig. 1). The comparison with experiment could be extended to the chemical shift anisotropy Δ_{cs} (vertical axis in Fig. 1). For this quantity, the agreement between theory and experiment is also very good, except for a single data point. However, we observe that if the sign of the anisotropy of this data point is inverted a good agreement is recovered with the calculated value for Se site 6 (cf. labeling of Ref. 12). Hence, we suggest that the experimental determination of the sign of this data point might have suffered from the noise in the spinning sidebands.¹⁰

In the adopted assignment, the Se sites 2 and 3, which are involved in ES tetrahedra, correspond to the isotropic shifts at 644 and 600 ppm, i.e., at higher shift values than all the other Se atoms which are involved in CS arrangements. This correspondence differs from the assignment proposed in Ref. 10, where it was argued that the ES shifts should occur on the opposite side of the range of measured chemical shifts. As can be inferred from the structural parameters reported in Table I, the chemical shift is found to be very sensitive to the mean Se-Ge distance and less so to the Ge-Se-Ge angle.

The structure of Ge_4Se_9 forms a layered structure similar to that of the GeSe_2 crystal.¹³ It only contains CS tetrahedra without any ES tetrahedra. However, one finds a Ge(3)-Se(6)-Se(7)-Ge(4) linkage, where the labeling corresponds to that of Ref. 13. In Fig. 2, the calculated results pertaining to each Se nucleus of the Ge_4Se_9 crystal are reported within

TABLE I. Calculated isotropic chemical shift δ_{iso} (ppm) and chemical shift anisotropy Δ_{cs} (ppm) are given for each Se nucleus in GeSe_2 , Ge_4Se_9 , GeSe , and Se crystals, successively. For GeSe_2 and Ge_4Se_9 , we adopt the labeling given in Refs. 12 and 13, respectively. Structural parameters such as the Ge-Se-Ge angle and the mean Se-Ge distance (in Å) are given. For GeSe_2 and Se , the experimental results are from Refs. 10 and 22, respectively. The asterisk indicates that the sign of the experimental anisotropy has been inverted.

Site	Experiment		Theory		Structure	
	δ_{iso}	Δ_{cs}	δ_{iso}	Δ_{cs}	\angle Ge-Se-Ge (deg)	Se-Ge
Se(1)	542	-400	585	-366	97.7	2.353
Se(2)	644	-550	685	-555	80.2	2.366
Se(3)	600	-350	625	-437	80.6	2.356
Se(4)	389	500	370	469	99.4	2.351
Se(5)	208	-350	133	-291	100.1	2.349
Se(6)	224	470*	143	375	98.3	2.349
Se(7)	396	500	413	526	96.2	2.357
Se(8)	515	-450	560	-347	96.3	2.359
Se(1)			382	348	97.3	2.354
Se(2)			203	-538	94.7	2.357
Se(3)			154	253	101.8	2.358
Se(4)			235	-431	98.9	2.342
Se(5)			447	343	97.4	2.356
Se(6)			453	417	91.3 ^a	2.363 ^b
Se(7)			536	425	91.1 ^a	2.367 ^b
Se(8)			247	-416	96.4	2.353
Se(9)			221	-338	100.6	2.357
Se			176	372	96.2, 103.5	2.571
Se	809		824	391		

^a \angle Se-Se-Ge.

^bMean of Se-Ge and Se-Se distances.

plots showing the chemical shift anisotropy Δ_{cs} vs the isotropic chemical shift δ_{iso} and compared to those of the GeSe_2 crystal. All the isotropic shifts of Ge_4Se_9 fall within the range

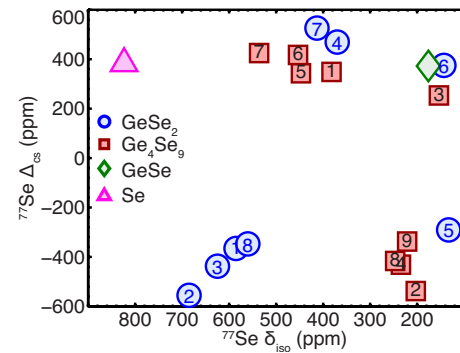


FIG. 2. (Color online) ^{77}Se chemical shift anisotropy (Δ_{cs}) vs isotropic shift (δ_{iso}) for calculated values for GeSe_2 (blue circles), Ge_4Se_9 (red squares), GeSe (green diamond), and Se (pink triangle) crystals. The labelings for GeSe_2 and Ge_4Se_9 correspond to those in Refs. 12 and 13, respectively.

TABLE II. Mean and range of ^{77}Se isotropic chemical shifts δ_{iso} (ppm) as found in the present calculations for GeSe_2 , Ge_4Se_9 , GeSe , and Se crystals. Five sites are distinguished.

Se site	Mean δ_{iso}	Range of δ_{iso}
Se-Se-Se	824	824
Ge-Se-Ge (ES)	655	625–685
Se-Se-Ge	495	453–536
Ge-Se-Ge (CS)	315	133–585
Threefold Se	176	176

of shifts corresponding to CS arrangements in the GeSe_2 crystal. This property also holds for the Se nuclei 6 and 7 belonging to Se-Se-Ge linkages, which are found at 453 and 536 ppm. Hence, this indicates that the contributions from CS and Se-Se-Ge arrangements overlap.

The atomic structure of the GeSe crystal consists of threefold Ge and threefold Se atoms.¹⁴ By symmetry, this structure only shows one inequivalent site for both Se and Ge. The corresponding calculated results have been added in the $\Delta_{\text{cs}}-\delta_{\text{iso}}$ plot in Fig. 2. This chemical shift lies at 176 ppm, suggesting that threefold coordinated Se sites contribute to

TABLE III. Calculated quadrupole coupling constant C_Q (MHz), isotropic chemical shift δ_{iso} (ppm), and chemical shift anisotropy Δ_{cs} (ppm) are given for each Ge nucleus in GeSe_2 , Ge_4Se_9 , GeSe crystals, successively.

Site	Structure	C_Q	δ_{iso}	Δ_{cs}
Ge(1)	ES	3.6	93	-241
Ge(2)	CS	-7.5	128	-130
Ge(3)	ES	3.1	108	-232
Ge(4)	CS	-11.9	132	-140
Ge(1)	CS	-8.0	126	-107
Ge(2)	CS	-13.6	141	-119
Ge(3)	Ge -Se-Se	4.7	160	134
Ge(4)	Ge -Se-Se	-5.2	157	134
Ge	Threefold	31.2	-82	-77

the low-value side of the range of chemical shifts originating from CS arrangements.

Our calculations for the GeSe_2 , Ge_4Se_9 , GeSe , and Se crystals give important indications for the interpretation of experimental ^{77}Se spectra of $\text{Ge}_x\text{Se}_{1-x}$ glasses. We distinguish five kinds of Se sites, corresponding to Se-Se-Se linkages, Ge-Se-Ge linkages in ES arrangements, Se-Se-Ge linkages, Ge-Se-Ge linkages in CS arrangements, and threefold coordinated Se sites. For each of these sites, we consider the average isotropic chemical shift and the observed range of values as they result from our calculations. Our assignments are summarized in Table II.

In Fig. 3, the structural assignments given in Table II are superposed to experimental spectra of ^{77}Se chemical shifts as obtained for $\text{Ge}_x\text{Se}_{1-x}$ glasses,^{9,10} leading to a globally consistent interpretation. Our assignments to Se-Se-Se linkages and Ge-Se-Ge linkages in CS arrangements fall in correspondence of the two dominating peaks at ~ 800 ppm and ~ 400 ppm, respectively, consistent with previous interpretations.^{9,10} Our study indicates that Se-Se-Ge linkages also contribute to the high-shift side of the peak at ~ 400 ppm, thereby giving overlapping contributions with those from Ge-Se-Ge linkages in CS arrangements. Hence, the location of the Se-Se-Ge contributions is in accord with the intuitive expectation that this line should lie in between those resulting from Se-Se-Se and Ge-Se-Ge linkages. The shoulder observed at ~ 650 ppm in Fig. 3(a) also lies in this intermediate range and closely corresponds in our description to ES arrangements. The present assignment of the ES line differs from that adopted in Ref. 10, where this line was situated on the low-shift side of the main peak. Finally, the contributions from threefold coordinated Se atoms are found on the low-shift side of the peak at ~ 400 ppm, in close correspondence of one of the Gaussian lines introduced in the experimental analysis of Ref. 10.

From the fit of the GeSe_2 spectrum in Ref. 10, one infers that 16% of the Se atoms contribute to the Gaussian line centered at 587 ppm. When this value is taken as an estimate for the fraction of Se atoms in ES arrangements, one finds consistency with the fraction of ES tetrahedra inferred from neutron-diffraction measurements (34%),⁴ which corre-

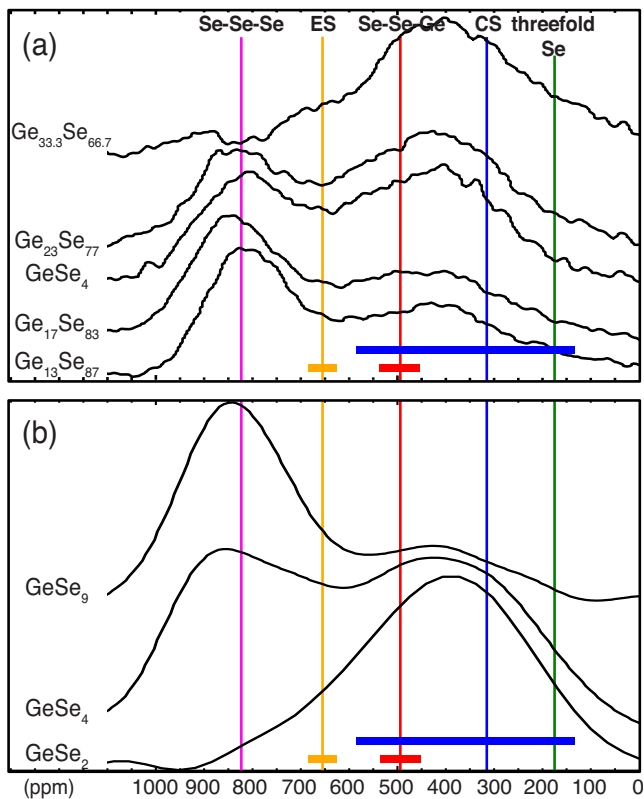


FIG. 3. (Color online) Average (vertical lines) and range (horizontal bar) of ^{77}Se isotropic chemical shifts for various Se sites as found from the present calculations (Table II), superposed to experimental results for $\text{Ge}_x\text{Se}_{1-x}$ glasses from (a) Ref. 10 and (b) Ref. 9. Five kinds of sites are distinguished: Se-Se-Se linkages (pink), Ge-Se-Ge linkages in ES arrangements (orange), Se-Se-Ge linkages (red), Ge-Se-Ge linkages in CS arrangements (blue), and threefold coordinated Se sites (green).

sponds to a fraction of 17% of Se atoms. As far as the Se-**Se**-Ge contributions are concerned, one notices that they fall in a region of the $\text{Ge}_x\text{Se}_{1-x}$ spectra where considerable intensity is observed. For GeSe_2 , this intensity could well account for the fraction of 20% of Se atoms involved in Se-Se bonds, which has been derived from neutron-diffraction measurements.⁴ As the Ge concentration in $\text{Ge}_x\text{Se}_{1-x}$ glasses drops, the intensity in the experimental spectra shifts from the peak at ~ 400 ppm (Ge-**Se**-Ge, CS) to the peak at ~ 800 ppm (Se-**Se**-Se) but the intensity corresponding to the lines assigned to ES and Se-**Se**-Ge arrangements remains sizable.

In anticipation of experiment, we complete this study by calculating the quadrupole coupling constant and chemical shifts for all ^{73}Ge nuclei of the considered crystals (Table III). We distinguish four kinds of Ge atoms. Following Ref. 27, the first two types correspond to tetrahedral arrangements, either CS or ES, with average chemical shifts of 132 ppm and 101 ppm, respectively. The third type corresponds

to Ge sites belonging to Ge-**Se**-Se linkages as found in the Ge_4Se_9 crystal, with an average chemical shift of 159 ppm. The last identified type is the threefold coordinated Ge, which has a chemical shift of -82 ppm in the GeSe crystal.

In conclusion, density-functional calculations of NMR parameters in various $\text{Ge}_x\text{Se}_{1-x}$ crystals were used for developing an assignment scheme relating chemical shifts to the underlying structure. Applied to ^{77}Se spectra of $\text{Ge}_x\text{Se}_{1-x}$ glasses, our assignment scheme provides an interpretation of the experimental data which is consistent with the occurrence of Ge-**Se**-Se linkages and does not require the notion of a bimodal phase.

We thank P. S. Salmon, S. E. Ashbrook, M. J. Duer, and S. Sen for useful interactions. We acknowledge the use of the Chemical Database Service at Daresbury (Ref. 28). Computing resources were provided by the Cambridge High Performance Computing Service HPCS and were funded by EPSRC under Grant No. EP/F032773/1.

-
- ¹A. Zakery and S. R. Elliott, *J. Non-Cryst. Solids* **330**, 1 (2003).
²K. Shimakawa, A. Kolobov, and S. R. Elliott, *Adv. Phys.* **44**, 475 (1995).
³L. Giacomazzi, C. Massobrio, and A. Pasquarello, *Phys. Rev. B* **75**, 174207 (2007).
⁴I. Petri, P. S. Salmon, and H. E. Fischer, *Phys. Rev. Lett.* **84**, 2413 (2000).
⁵D. N. Tafen and D. A. Drabold, *Phys. Rev. B* **71**, 054206 (2005).
⁶C. Massobrio and A. Pasquarello, *Phys. Rev. B* **77**, 144207 (2008).
⁷C. Massobrio, M. Celino, P. S. Salmon, R. A. Martin, M. Micoulaud, and A. Pasquarello, *Phys. Rev. B* **79**, 174201 (2009).
⁸B. Bureau, J. Troles, M. Le Floch, F. Smektala, and J. Lucas, *J. Non-Cryst. Solids* **326-327**, 58 (2003).
⁹P. Lucas, E. A. King, O. Gulbilen, J. L. Yarger, E. Soignard, and B. Bureau, *Phys. Rev. B* **80**, 214114 (2009).
¹⁰E. L. Gjersing, S. Sen, and B. G. Aitken, *J. Phys. Chem. C* **114**, 8601 (2010).
¹¹J. Akola and R. O. Jones, *Phys. Rev. Lett.* **100**, 205502 (2008).
¹²G. Dittmar and H. Schafer, *Acta Crystallogr., Sect. B: Struct. Crystallogr. Cryst. Chem.* **32**, 2726 (1976).
¹³J. E. Kwak and H. Yun, *Acta Crystallogr., Sect. C: Cryst. Struct. Commun.* **61**, i81 (2005).
¹⁴H. Wiedemeier and H. G. V. Schnering, *Z. Kristallogr.* **148**, 295 (1978).
¹⁵C. J. Pickard and F. Mauri, *Phys. Rev. B* **63**, 245101 (2001).
¹⁶S. J. Clark, M. D. Segall, C. J. Pickard, P. J. Hasnip, M. J. Probert, K. Refson, and M. C. Payne, *Z. Kristallogr.* **220**, 567 (2005).
¹⁷J. R. Yates, C. J. Pickard, and F. Mauri, *Phys. Rev. B* **76**, 024401 (2007).
¹⁸D. Vanderbilt, *Phys. Rev. B* **41**, 7892 (1990).
¹⁹J. P. Perdew, K. Burke, and M. Ernzerhof, *Phys. Rev. Lett.* **77**, 3865 (1996).
²⁰H. J. Monkhorst and J. D. Pack, *Phys. Rev. B* **13**, 5188 (1976).
²¹R. Keller, W. B. Holzapfel, and H. Schulz, *Phys. Rev. B* **16**, 4404 (1977).
²²M. Gopal and J. Milne, *Inorg. Chem.* **31**, 4530 (1992).
²³V. K. Michaelis, P. M. Aguiar, V. V. Terskikh, and S. Kroeker, *Chem. Commun. (Cambridge)* **2009**, 4660.
²⁴M. Kibalchenko, J. R. Yates, and A. Pasquarello, *J. Phys.: Condens. Matter* **22**, 145501 (2010).
²⁵H. M. Petrilli, P. E. Blöchl, P. Blaha, and K. Schwarz, *Phys. Rev. B* **57**, 14690 (1998).
²⁶P. Pyykkö, *Mol. Phys.* **106**, 1965 (2008).
²⁷S. Sugai, *Phys. Rev. B* **35**, 1345 (1987).
²⁸D. Fletcher, R. McMeeking, and D. Parkin, *J. Chem. Inf. Comput. Sci.* **36**, 746 (1996).